

Supporting Information for:

Size-Dependent Phase Transfer Functionalization of Gold Nanoparticles to Promote Well-Ordered Self- Assembly

Florian Schulz,^{,†,‡} Steffen Tober,^{†,¶} Holger Lange^{†,‡}*

[†] Institute for Physical Chemistry, University of Hamburg, Grindelallee 117, 20146 Hamburg,
Germany.

[‡] The Hamburg Centre for Ultrafast Imaging (CUI), Luruper Chaussee 149, 22761 Hamburg,
Germany.

[†] present address: Deutsches Elektronen-Synchrotron DESY, Notkestr. 85, 22607 Hamburg,
Germany

Additional experimental information

Materials. Tetrachloroauric(III) acid ($\geq 99.9\%$ trace metal basis), trisodium citrate dihydrate ($\geq 99.0\%$), acetone and propan-2-ol were ordered from Sigma-Aldrich. Ethylenediaminetetraacetic acid tetrasodium salt hydrate (EDTA), sodium hydroxide solution ($c(\text{NaOH}) = 1 \text{ mol/L}$, 1 N) and citric acid monohydrate ($\geq 99.5\%$) were obtained from Merck. Ultrapure water was used for all procedures.

Synthesis of AuNP >12 nm. AuNP with 12.3 nm diameter were synthesized and characterized as described previously.¹ These AuNP were used as seeds to synthesize larger AuNP with a seeded growth protocol based on the one described by Bastús et al.² To this end the pH of 900 mL seed particles was raised by addition of sodium hydroxide solution (3 mL, 4%, 1N). For one growth step, EDTA (50 μL , 100 mM), trisodium citrate dihydrate (13 mL, 75 mM), water (100-150 mL) and finally tetrachloroauric acid (6.5 mL, 25 mM) were added at 80 °C and the mixture reacted for 45 minutes. Then, 100 mL of the AuNP solution was removed. With the remaining solution ($V \sim 900 \text{ mL}$ considering evaporation losses) this was repeated 6 times, yielding AuNP up to 29 nm in diameter. In the following steps the addition of EDTA was increased to 62.5 μL in each step, and trisodium citrate dihydrate solution (13 mL) was added only every third step. 13 additional steps yielded AuNP with 56 nm in diameter. Sodium hydroxide solution (3.25 mL, 4%, 1N) was added and ten additional steps yielded AuNP with 90 nm in diameter. Overall, the synthesis yields 100 mL AuNP in each step with 2-3 nm increase of diameter in each step. The dispersity of diameters ranged from 6-10 %.

These citrate-stabilized AuNP were characterized with TEM as described previously.^{1,3} The diameters of the selected AuNP@Citrate used for the study are the AuNP-core diameters determined by TEM-analysis: $12.3 \pm 0.8 \text{ nm}$, $23.1 \pm 2.1 \text{ nm}$, $40.0 \pm 3.1 \text{ nm}$, $46.8 \pm 3.3 \text{ nm}$, $61.3 \pm 6.4 \text{ nm}$, $79.6 \pm 5.9 \text{ nm}$ and $89.8 \pm 7.8 \text{ nm}$.

Synthesis of small AuNP: The protocol by Piella et al.⁴ was upscaled by a factor of 6. A heating plate instead of the heating mantle and a beaker covered with aluminium foil instead of a three-neck flask was used. To provide better mixing conditions, a diluted tetrachloroauric acid precursor (106 mL, 1.4 mM) was used. Aqueous trisodium citrate dihydrate (800 mL, 2.475 mM) was heated with aqueous tannic acid (0.6 mL, 2.5 mM) and potassium carbonate (6 mL, 150 mM). When the reaction volume reached 70 °C, the pre-heated precursor was injected. After 15 minutes the reaction was completed and the AuNP were removed for storage. A mean core diameter of $6.4 \pm 1.1 \text{ nm}$ was determined by TEM-analysis.

AuNP@OLAM films: Silicon wafers were cut into approximately 5x5 mm pieces and cleaned by subsequent sonication in water, acetone and propan-2-ol for at least 10 minutes per step. For film synthesis, the wafers were fully covered with 5 μL or 10 μL AuNP solution. Experiments were conducted with approximately 0.5 μM AuNP@OLAM with $d_{\text{AuNP}} = 12 \text{ nm}$ and 6.7 μM AuNP@OLAM with $d_{\text{AuNP}} = 6.4 \text{ nm}$ in toluene.

Scanning electron microscopy (SEM): A GEMINI LEO 1150 operating at 20.0 kV was used for analysis of AuNP@OLAM films on silicon wafers. The electron microscopy data were analyzed with Image J v1.50i.

Grazing incidence small-angle x-ray scattering (GISAXS): Selected films were analyzed by GISAXS. The setup consisted of an Incoatec X-ray source I μ S with Quazar Montel optics, a variable evacuated flight tube (used at 1 m) and a Rayonix SX165 CCD detector. The incident angle was 0.1°, accumulation time of the measurement was 1200 s for AuNP@OLAM with $d_{\text{AuNP}} = 12$ nm and 600 s for those with $d_{\text{AuNP}} = 6.4$ nm. The scattering data were analyzed with Scatter v2.5.⁵

Kinetics of indirect functionalization: 10 mL AuNP@OLAM with core diameters 6.4 nm and 12.3 nm were prepared as described. The organic phase was extracted and filtered. To reduce the concentration of free oleylamine, parts of the solution were centrifuged at 20,000 g for 30 minutes ($d_{\text{AuNP}} = 12.3$ nm) or 60 minutes ($d_{\text{AuNP}} = 6.4$ nm). Afterwards 0.9 mL of the supernatants were replaced by toluene and the particles were redispersed by sonication. UV/Vis spectra of 0.84 mL AuNP@OLAM were collected before addition of 0.16 mL of the secondary ligand solutions (PSSH2k, 5k or 10k, 1 mM in toluene), 15 s after addition and afterwards in intervals of 2 minutes within the first hour.

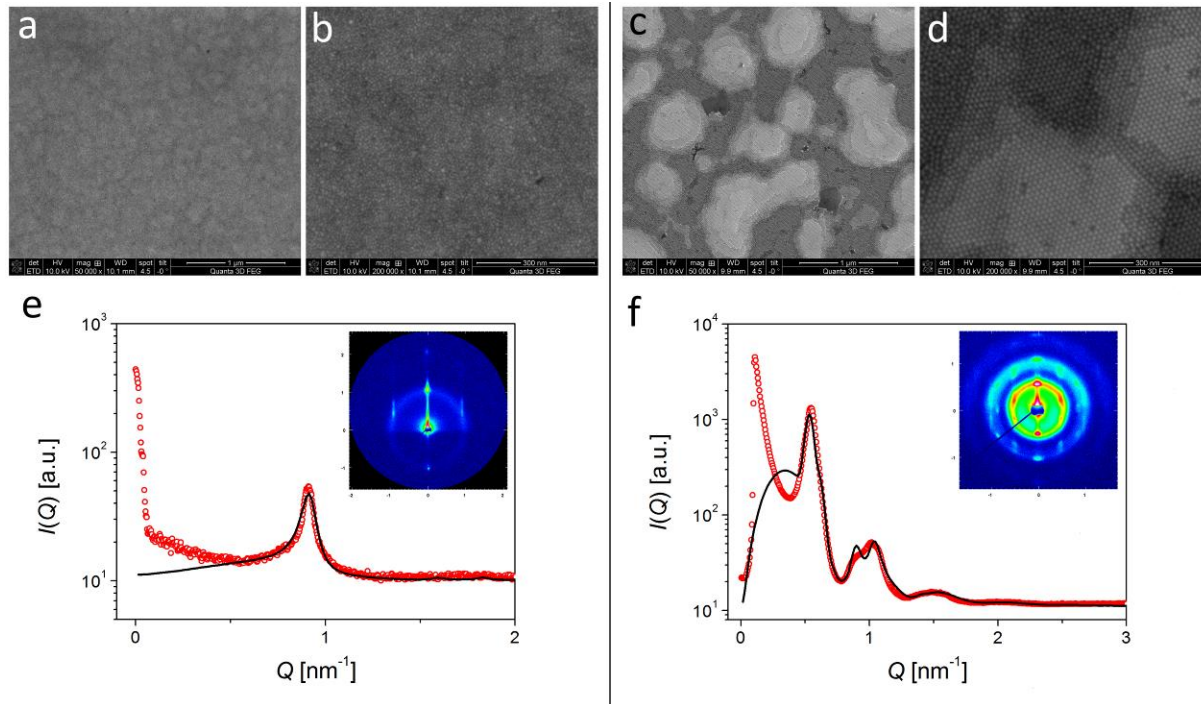


Figure S1. Exemplarily measurements of dried AuNP@OLAM films. SEM measurements of AuNP@OLAM with $d_{\text{AuNP}} = 6.4$ nm, $c(\text{AuNP}) = 6.7$ μM (a and b) and $d_{\text{AuNP}} = 12.3$ nm, $c(\text{AuNP}) = 0.52$ μM (c, d) dropcasted onto silicon wafers. The dried films of the smaller AuNP@OLAM were less ordered and the according scattering intensity profiles could be fitted with a 2D-hexagonal lattice model as shown in e, the inset shows the scattering pattern. The films of the larger AuNP were sufficiently thick to fit the scattering data with a fcc-model (f, scattering pattern in the inset). The obtained radii, dispersities and interparticle distances agree well with the ones obtained by TEM and SEM-analysis.

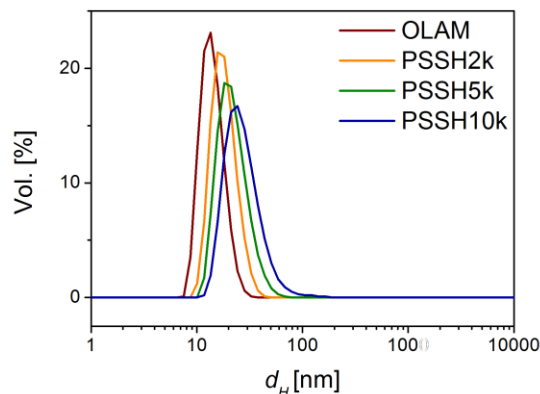


Figure S2. Volume-weighted distributions of hydrodynamic diameters d_H obtained by DLS for AuNP@OLAM (TEM: $d_{\text{AuNP}} = 11.9$ nm) reacted with PSSH ligands as indicated. The volume weighted mean d_H were: $d_H(\text{AuNP@OLAM}) = 14.3$ nm, $d_H(\text{AuNP@PSSH2k}) = 18.5$ nm, $d_H(\text{AuNP@PSSH5k}) = 22.5$ nm and $d_H(\text{AuNP@PSSH10k}) = 28.6$ nm.

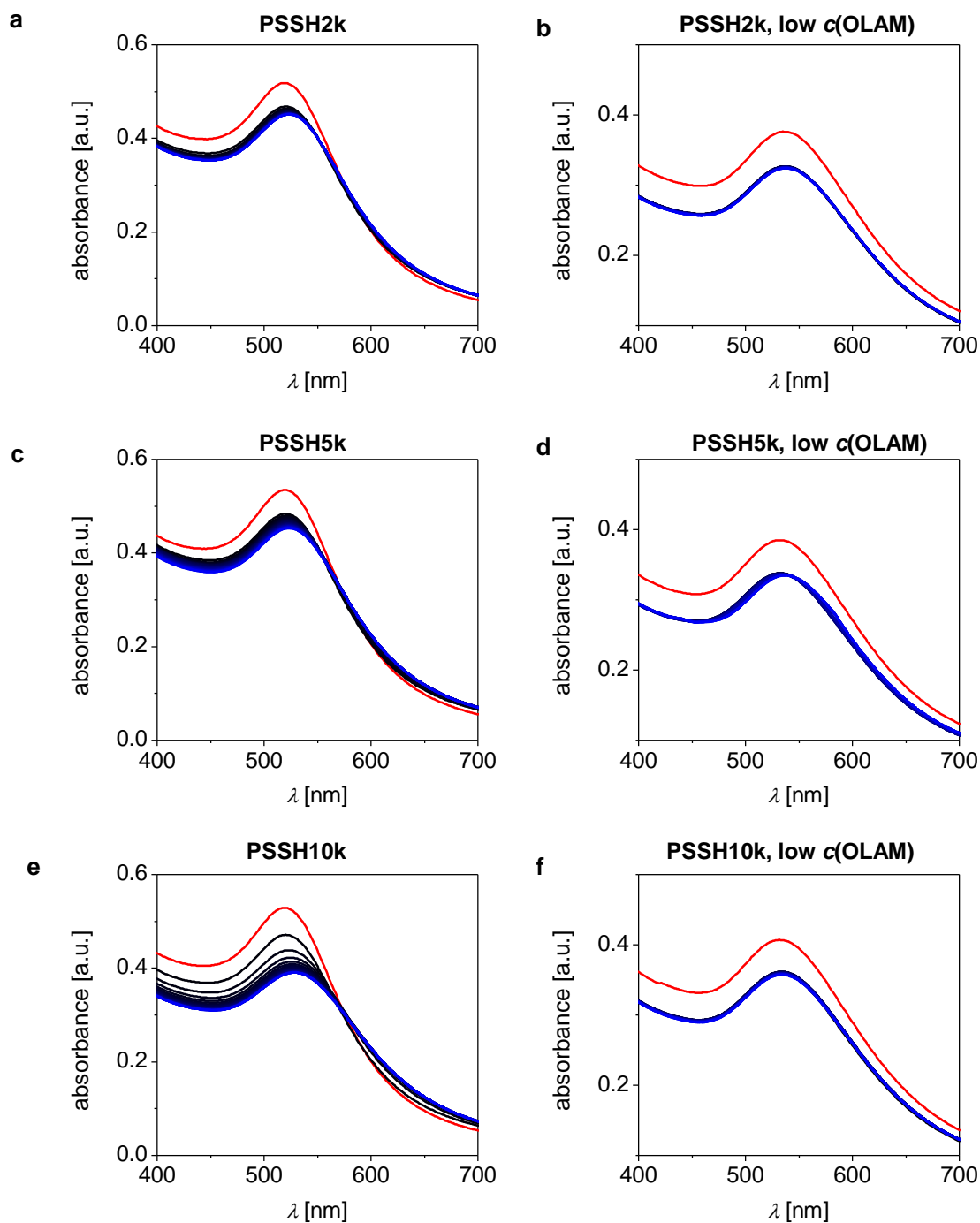


Figure S3. Absorbance spectra of AuNP@OLAM ($d_{\text{AuNP}} = 6.4$ nm) reacted with PSSH ligands in toluene. The spectra before PSSH addition are also shown (red lines). After addition of PSSH solutions (to yield 0.16 mM), 30 absorbance spectra were recorded in intervals of 2 minutes (dark blue to blue lines). Indications of slight aggregation (broadening and redshift of the localized surface plasmon resonance band, LSPR) are more pronounced for increasing ligand sizes (a: PSSH2k, c: PSSH5k, e: PSSH10k). When the concentration of free OLAM is reduced by a factor of ten, no indications of aggregation are observed (b: PSSH2k, d: PSSH5k, f: PSSH10k).

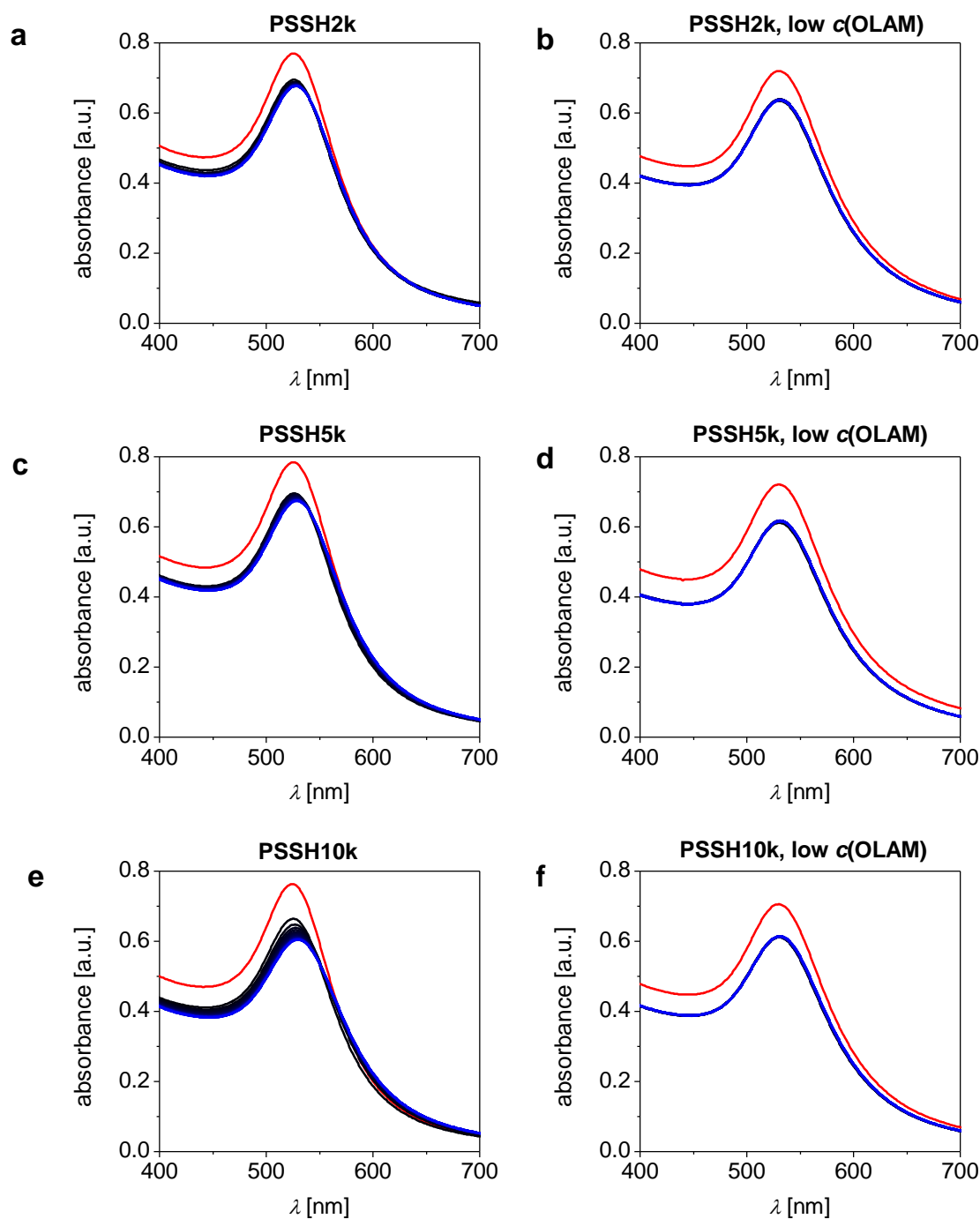


Figure S4. Absorbance spectra of AuNP@OLAM ($d_{\text{AuNP}} = 12.3$ nm) reacted with PSSH ligands in toluene. The spectra before PSSH addition are also shown (red lines). After addition of PSSH solutions (to yield 0.16 mM), 30 absorbance spectra were recorded in intervals of 2 minutes (dark blue to blue lines). The same observations as described in Figure S5 were made, but the aggregation seems to be less pronounced (**a**: PSSH2k, **c**: PSSH5k, **e**: PSSH10k). As for the smaller AuNP, with reduced free OLAM concentration no indications of aggregation are observed (**b**: PSSH2k, **d**: PSSH5k, **f**: PSSH10k).

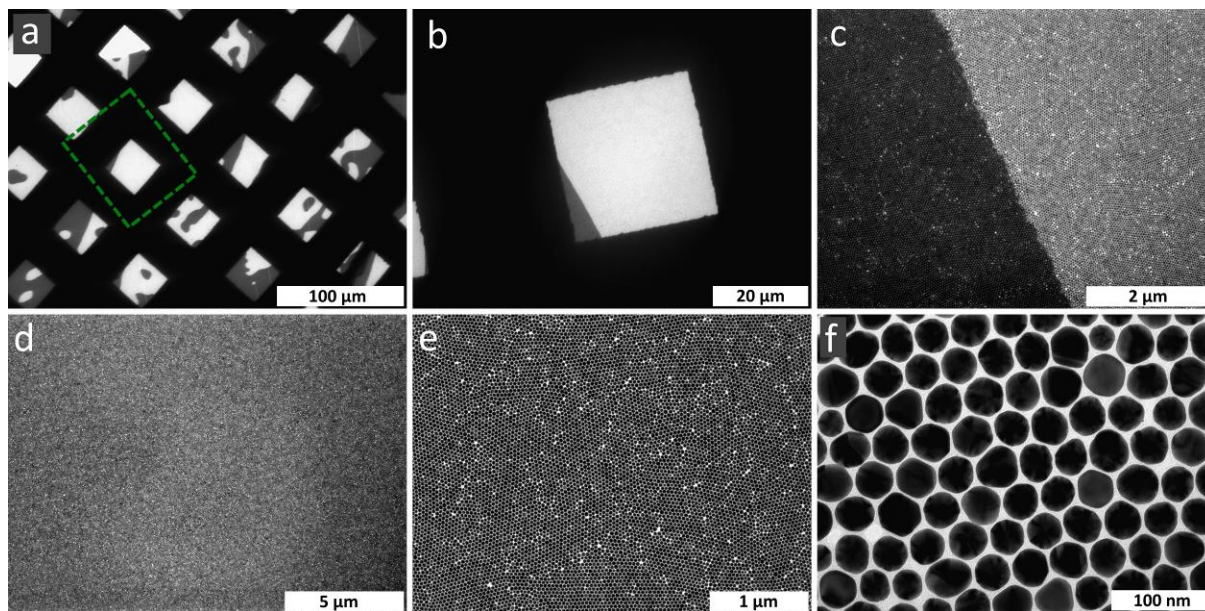


Figure S5. TEM-images of self-assembled AuNP@PSSH2k ($d_{\text{AuNP}} = 36$ nm). **a:** Large area view of self-assembled AuNP@PSSH2k. The light grey areas are monolayers, the darker regions consist of bi- or multiple layers. **b:** magnification of the highlighted area in **a** showing a mesh completely covered with a monolayer except the small darker area in the lower left corner. **c:** magnification of the lower left corner in **b**. Lower panel **d**, **e**, **f:** Exemplarily magnifications of the light grey area in **b**.

REFERENCES

- (1) Schulz, F.; Homolka, T.; Bastús, N. G.; Puentes, V.; Weller, H.; Vossmeier, T. Little Adjustments Significantly Improve the Turkevich Synthesis of Gold Nanoparticles. *Langmuir* **2014**, *30*, 10779–10784.
- (2) Bastús, N. G.; Comenge, J.; Puentes, V. Kinetically Controlled Seeded Growth Synthesis of Citrate-Stabilized Gold Nanoparticles of up to 200 nm: Size Focusing versus Ostwald Ripening. *Langmuir* **2011**, *27*, 11098–11105.
- (3) Schulz, F.; Vossmeier, T.; Bastús, N. G.; Weller, H. Effect of the Spacer Structure on the Stability of Gold Nanoparticles Functionalized with Monodentate Thiolated Poly(ethylene glycol) Ligands. *Langmuir* **2013**, *29*, 9897–9908.
- (4) Piella, J.; Bastús, N. G.; Puentes, V. Size-Controlled Synthesis of Sub-10-nanometer Citrate-Stabilized Gold Nanoparticles and Related Optical Properties. *Chem. Mater.* **2016**, *28*, 1066–1075.
- (5) Förster, S.; Apostol, L.; Bras, W. Scatter: Software for the analysis of nano- and mesoscale small-angle scattering. *J. Appl. Crystallogr.* **2010**, *43*, 639–646.